An alternative kinetic approach to describe the isothermal pyrolysis of micro-particles of sugar cane bagasse

Joan J. Manyà [*], Jesús Arauzo

*Thermo-chemical Processes Group (GPT), Aragón Institute of Engineering Research (I3A), University of Zaragoza,
Maria de Luna 3, E-50018 Zaragoza, Spain*

Abstract

A new kinetic approach is presented for modeling micro-particle pyrolysis of sugar cane bagasse for isothermal conditions. The model is based on a superimposition of kinetics pseudo-components which are based on single-step reactions to model primary pyrolysis. To ensure the validity and reliability of the kinetic parameters, the operating conditions must guarantee the minimisation of heat transfer intrusions and vapour–solid interactions.

The kinetic model was previously deduced from thermogravimetric data obtained at $20\,K\,min^{-1}$ for the same bagasse samples. The potential effects related to an increase of the heating rate and the mineral matter content were taken into account during the adjustment of the parameters to reproduce the isothermal experiments.

A generalised kinetic model proposed by Miller and Bellan [R.S. Miller, J. Bellan, A generalised biomass pyrolysis model based on superimposed cellulose, hemicellulose and lignin kinetics, Combust. Sci. Technol. 126 (1997) 97–137] was selected to compare the degree of agreement between the two models. In spite of the effectiveness of the Miller and Bellan model, a slightly better performance was achieved for the model proposed in this work.

The methodology followed in the present study for sugar cane bagasse samples could be useful to predict the isothermal pyrolysis behaviour of arbitrary biomass feedstocks in a relatively easy way.
© 2007 Elsevier B.V. All rights reserved.

Keywords: Pyrolysis; Isothermal; Sugar cane bagasse; Kinetics

1. Introduction

Pyrolysis of biomass appears within the most promising conversion routes of waste upgrading. This process provides several benefits compared to conventional combustion, with very promising feedstock availability and products applications. Also the most important system aspects (like cost reduction potential, integration into the energy system, and environmental benefits) are advantageous.

The development of thermochemical processes for biomass conversion requires the knowledge of the most significant pyrolysis kinetic parameters. As far as empirical modeling concerns, the main proposed kinetic mechanisms are based either on a one step reaction (global decomposition) or on several competitive parallel reactions.

The mechanisms of global decomposition describe the thermal degradation by means of an irreversible and single-step reaction [1] to predict the overall rate of volatiles release (i.e., mass loss), but without separately predict the production of condensable and gas from volatile product. Usually the mass loss rate is described by models assuming biomass as the sum of pseudo-components, or fractions of the biomass components decomposing in similar way and in similar temperature ranges [2–7]. The corresponding experimental studies have been mostly carried out with small particles, employing thermogravimetric systems. These models have the particularity of predicting constant char for all temperatures.

On the other hand, the formulation of kinetic models based on competitive, parallel, irreversible and first-order reactions allow to get an estimation of the different fractions of pyrolysis products [8–15]. These models are known as "Broido-Shafizadeh models", and are based on a distributive approach of the process.

Nomenclature

A	pre-exponential factor (s^{-1})
c	mass fraction of the biomass components in the virgin material
E	apparent activation energy ($J\,mol^{-1}$)
k_1, k_2, k_3	kinetic constants of the MB model
m_0	initial dry sample mass (mg)
N	number of data points
S_{TG}	sum of the quadratic deviations between the experimental values and the simulated ones from the kinetic models
t	time (s)
T	temperature (K)
T_1	measured temperature inside the sample (K)
T_{peak}	temperature value corresponding to the maximum weight-loss rate (K)
T_1^*	required temperature inside the sample (K)
V	accumulated production of volatile matter (mg)
V^*	final accumulated production of volatile matter (mg)
x	char production mass ratios in the MB kinetic scheme
x_{ext}	mass fraction of extractives in the virgin material
y_a	weight fraction of activate component (MB model)
y_c	weight fraction of char product (MB model)
y_{comp}	weight fraction of virgin component (MB model)
y_g	weight fraction of gas product (MB model)
y_t	weight fraction of condensable product (MB model)
w	residual weight fraction in moisture-free basis

Greek letters

α	mass fraction of volatiles at time t
η	experimental char yield (mass fraction)
τ	solid residence time (min)

In the majority of the cases, these mechanisms have not been validated by thermogravimetry or under conditions assuring kinetic control.

The mineral matter naturally present in the biomass catalyses the pyrolytic decomposition in an unpredictable variety of ways [16]. Previous studies [17,18] showed that thermogravimetric analysis of small samples of lignocellulosic materials at low (below 5 K min^{-1}) to moderate (below 100 K min^{-1}) heating rates usually evidences a distinct DTG (differential weight loss curve) peak resulting from the decomposition of cellulose, a lower temperature process associated to hemicellulose pyrolysis, and an attenuated shoulder that can be attributed to lignin decomposition. This is because lignin decomposes slowly over a very broad range of temperatures, providing a gently sloping baseline to the DTG curve [19]. Sometimes the first peaks merge into one very broad peak because the mineral matter present in the biomass samples can highly increase the overlap of the

partial peaks in DTG curves [18]. Later several other studies evidenced the ability of pre-treatments to separate merged peaks, displace reaction zones toward higher temperatures, decrease char yield and increase peak reaction rates [6,20–23]. Of these pre-treatments, the water washing is preferred because it results in less hydrolysis and solubilisation of the holocellulose [1].

Experimental measurements of the pyrolytic behaviour of biomass at high-heating rates have been the focus of extraordinary interest in the research community, but practical problems associated with these measurements have often been overlooked. The most important errors are connected to problems of temperature measurements and to the self-cooling/self-heating of samples due to heat demand by the chemical reaction. A consequence of these limitations is that the single-step activation energy measured at high-heating rates is almost always lower than its true value [1]. Another consequence is that weight loss is reported at temperatures much higher than it actually occurs [1,6]. For these reasons, extensive investigations have not yielded a satisfactory pyrolysis model capable of predicting the mass loss obtained over wide ranges of pyrolysis conditions [1,12,24].

The present study is focused on the pyrolysis of sugar cane bagasse samples under different heating conditions: slow heating rate (thermogravimetric experiments) and fast heating rate (experiments performed in a micro-reactor at isothermal conditions). A new kinetic modeling approach is proposed in order to predict the primary biomass decomposition behaviour over a wide temperature range and under both isothermal and non-isothermal regimes.

2. Experimental

2.1. Samples

The samples of sugar cane bagasse used in the study were obtained as a dried, fibrous product from the sugar factory of Ingenio Concepcion. This plant is located in the region of Tucuman (Republic of Argentina). The material was crushed and sieved to provide a feed sample in the size comprised in the range from 0.25 mm to 1 mm.

According to the procedure suggested by other authors [1,2], the biomass samples were washed with hot water in order to partly remove the inorganic matter. Much of the potassium and sodium present in biomass can be readily removed in this way [25]. The water wash is preferred over acid washes because it results in less hydrolysis and solubilisation of the holocellulose. Both a cold and a hot wash were used. In the cold wash, 1 g of sample was placed in 200 ml deionised water and stirred for 20 h at room temperature, then filtered and washed with 300 ml H_2O. In the hot wash, 1 g of sample (previously washed with cold water) was placed in 120 ml deionised water and stirred for 2 h at 353 K, then filtered and washed with 300 ml H_2O.

The untreated samples of bagasse were extracted with ethyl alcohol (for about 24 h in a Soxhlet apparatus) following a standard methodology for the determination of extractives in biomass [26]. The extractives content was 2.1% (by weight).

Table 1
Analysis of sugar cane bagasse samples

Proximate analysis (%)	Analytical standard	Untreated sugar cane bagasse	Washed sugar cane bagasse
Moisture	ISO-589-1981	2.20	3.99
Ash	ISO-1171-1976	5.02	3.32
Volatiles	ISO-5623-1974	74.98	76.18
Fixed carbon	By difference	17.80	16.51
Ultimate analysis (%dry ash free basis)	Analytical instrument	Untreated sugar cane bagasse	Washed sugar cane bagasse
Carbon	Carlo Erba 1108	43.60	44.48
Hydrogen	Carlo Erba 1108	5.52	5.70
Nitrogen	Carlo Erba 1108	0.25	0.19
Sulphur	Carlo Erba 1108	0.07	<0.05
Oxygen	By difference	50.63	49.63

Proximate and ultimate analyses of the sugar cane bagasse samples are shown in Table 1. Additionally, Table 2 reports the results corresponding to the analysis of the bagasse ashes by X-ray fluorescence spectroscopy (XRF). A semi-quantitative standard XRF analysis was made using a Philips PW 2400 spectrophotometer and a rhodium anode X-ray tube.

2.2. Thermogravimetric apparatus

The TGA equipment consisted of a Cahn TG-151 thermobalance (vertical balance, $10\,\mu g$ resolution, 1373 K maximum temperature at atmospheric pressure, 70 bar maximum pressure at 1273 K, and $25\,K\,min^{-1}$ maximum heating rate). Non-isothermal experiment runs were carried out at $20\,K\,min^{-1}$ under atmospheric pressure, with an initial weight sample of 10 mg and with a nitrogen purge flow of $200\,cm^3\,min^{-1}$ (normal conditions) to remove vapour pyrolysis products. The final temperature corresponded to 1173 K. The crucible was open at the top and made of ceramic material with the purpose of minimising the mass-transfer limitations. At least three runs

were carried out for each material (unwashed and washed bagasse).

2.3. Micro-reactor system

To obtain an isothermal mass-change determination curve for a given material, at a given operating temperature (T_1^*), several bagasse samples were placed, one at a time, into a constant-temperature inert atmosphere for a given length of time. The weight changes were measured on a common laboratory balance.

The isothermal experiments were performed in a device designed for this purpose. It is a modification and improvement of the pyrolysis system used by Thurner and Mann [9]. Fig. 1 shows a schematic diagram of the experimental system. The reactor consisted of a reaction chamber, a cooler, and a condenser. The reaction chamber was made of a 38.1 mm schedule 40 stainless steel tube (ASTM N08904). This tube was heated by two semi-cylindrical electrical heating units having a total power of 1 kW. The temperature inside the chamber was measured with a thermocouple (type K) and regulated by a PID controller.

The device provided an isothermal reaction zone at least 8 cm long (a maximum temperature difference of 5 K and negligible radial temperature dispersion) and two zones of low temperature. The cooled zone 1 was used to maintain the sample at low temperature (below 313 K) before it was inserted into the pyrolysis chamber and to cool it down quickly at the end of a run. The sample material was placed in a stainless steel wire mesh basket soldered to a metallic rod, which could easily move horizontally inside the reactor tube. A fine thermocouple (1.5 mm diameter, type K) was embedded in the middle of the sample basket to measure the reaction temperature accurately inside the sample.

A flow rate of $3\,dm^3\,min^{-1}$ of helium (measured at 298 K and 101.3 kPa) was chosen in order to maintain a uniform temperature zone, displace the oxygen from the reactor and carry away the volatile and gaseous products. The only reason for using helium instead of nitrogen is the reduction of the temperature gradients in the reactor chamber (the mean specific heat of nitro-

Table 2
Analysis of sugar cane bagasse ashes by XRF

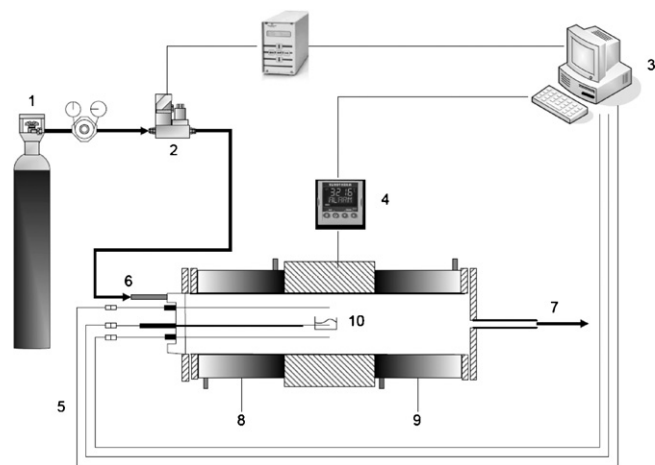| Oxide (%ash)	Untreated sugar cane bagasse	Washed sugar cane bagasse	Difference (%)
SiO_2	64.29	74.24	15.5
CaO	4.84	6.16	27.3
K_2O	14.34	2.20	−84.7
MgO	1.33	1.59	19.5
Fe_2O_3	3.69	5.54	50.1
P_2O_5	2.89	1.12	−61.2
Al_2O_3	3.44	2.70	−21.8
SO_3	0.97	0.45	−53.6
TiO_2	1.25	1.92	53.6
ZnO	1.06	1.62	52.8
Cr_2O_3	0.54	0.77	42.6
CuO	0.51	0.75	44.4
Na_2O	0.31	0.08	−74.2
MnO_2	0.54	0.83	53.7
BaO	0.07	0.01	−85.7
Undetermined	−0.07	0.02	

Fig. 1. Experimental system for isothermal mass-change determination. (1), inert gas; (2), mass flow controller; (3), data acquisition; (4), furnace temperature controller; (5), thermocouples; (6), helium input; (7), gas output; (8), cooler; (9), condenser; (10), sample basket.

gen is higher than helium in the temperature range considered and, additionally, helium has a higher thermal conductivity). Untreated and washed sugar cane bagasse particles (initial mass sample of around 115 mg) were tested at reactor temperatures of 548, 573, 598, 623, 648, 673, 723, 773, and 873 K. Additionally, the isothermal experiments were carried out at three different values of solid residence time (τ): 3, 6, and 8 min. A preliminary study of the thermal history of the experimental system (using an empty sample basket) has allowed estimating the time needed to reach the temperature set point (T_1^*). This time was approximately 30 s setting T_1^* value at 873 K. On the other hand, the temperature profile obtained for 150 mg of pine charcoal was relatively similar to that obtained using an empty sample basket. These results could be considered as expected because the dimensions of the packed bed are very small compared to those of the heated zone. For these reasons, it is reasonable to assume that the heat transfer limitations are not critical for the biomass samples used in the present study. In accordance with this assumption, simultaneous TGA/DSC experiments performed by Stenseng et al. [27] showed that a biomass sample (straw) presents much lower heat demand than pure cellulose (Avicel) and, consequently, it is less affected by heat transfer intrusions.

3. Kinetic approach

A viable kinetic scheme for the pyrolysis of micro-particles must accurately predict the temporal mass evolution and the char yield variations with temperature, heating conditions, and biomass feedstock. "Micro-particles" pyrolysis involves the thermal decomposition of materials with sample sizes sufficiently small such that diffusion effects become negligible and the process becomes kinetically controlled. Critical particle size estimates for kinetic control are generally below 1 mm [13,24,28–30].

Várhegyi et al. [18] suggest that both kinetic schemes and parameters are necessary for each heating rate, thermal pretreatment (moisture removal) and mineral content studied. This scenario could invalidate the usefulness of the experimental results as it does not provide reliability to use them for untested conditions. However, and as already suggested by Miller and Bellan [14], this is the rationale of kinetic approaches: once determined from a finite number of experiments, it can be used for all conditions without taking into consideration the heating rate and/or other related effects. Nevertheless, this objective seems difficult to reach because the complexity of the process and its dependence on thermal conditions and biomass type, among others. For this reason, it is necessary to develop kinetic approaches which represent a compromise between scientific rigour and practical considerations.

The above-mentioned considerations have been taken into account to develop a new kinetic approach. The experimental weight loss evolutions obtained from isothermal experiments were simulated using a kinetic model based on superimposed pseudo-components and previously deduced from thermogravimetric data. Taking into account that the kinetic model has been deduced from non-isothermal experiments performed in

the TGA apparatus, some model kinetic parameters need to be adjusted to reproduce the isothermal experiments. However, the adjustment of the kinetic parameters was based on the current state of knowledge regarding this topic. In this sense, only values corresponding to char yields and pre-exponential factors can be modified. The use of low-heating rate TGA experiments causes difficulties in distinguishing between the high- and low-temperature contributions to the pyrolysis. In fact, kinetics derived from TGA studies generally predict large char yield [14]. On the other hand, the adjustment of the pre-exponential factor becomes an effective way to minimise the impact of the thermal lag (i.e., the difference between the true sample temperature and the measured temperature) when the heating rate is increased [31].

The reliability of this study depends on the assumption that the role of secondary reactions is negligible. It is well reported that char is formed through secondary reactions between vapour products catalysed by contact with the solid matrix [1,18,20,32].

In order to check the ability of the model proposed in this work to predict the isothermal mass-change curve, another kinetic model has been analysed to compare the degree of agreement between the two alternatives. The model selected for this comparison was a generalised biomass pyrolysis model proposed by Miller and Bellan (MB) [14]. In the MB kinetic scheme, the pyrolysis of general biomass materials is modeled via a superposition of cellulose, hemicellulose and lignin kinetics. All three of the primary biomass components are modeled with multi-step kinetics involving competitive primary decomposition reactions.

4. Results and discussion

4.1. Kinetic model validation from thermogravimetric data

The total weight loss associated to the pyrolysis process of the samples under study was simulated assuming the addition of the three-independent parallel devolatilisation reactions, corresponding to three pseudo-components linked to the hemicellulose, cellulose and lignin. This model, proposed in a previous study [6], has been proven effective to describe the global mass loss during pyrolysis of several biomasses [7]. The mathematical expression of the kinetic model is as follows:

$$\frac{d\alpha}{dt} = \sum_{i=1}^{3} A_i \exp\left[\frac{-E_i}{RT}\right] f(\alpha_i) \quad (1)$$

where α is the fraction of volatiles at time t, E the apparent activation energy, and A is the pre-exponential factor. The subscripts i refer to the three following pseudo-components: (a) $i = 1$, a hemicellulose fraction that decomposes in the low-temperature range; (b) $i = 2$, a cellulose fraction that decomposes in the mid-temperature range; (c) $i = 3$, the fraction of lignin present plus extractives and the remaining amounts of holocellulose.

In this study, experimental values were correlated using the model expressed as a function of the volatile matter accumulated production (V). The kinetic model is based on the assumption of an irreversible, single-step, first-order process for each pseudo-

component, except for the third one, for which a kinetic model of third order is applied.

$$\frac{\mathrm{d}V}{\mathrm{d}t} = A_1 \exp\left[\frac{-E_1}{RT}\right](V_1^* - V_1) + A_2 \exp\left[\frac{-E_2}{RT}\right](V_2^* - V_2)$$

$$+ A_3 \exp\left[\frac{-E_3}{RT}\right]\frac{(V_3^* - V_3)^3}{V_3^{*2}} \qquad (2)$$

The parameter V^* corresponds to the final accumulated production of volatile matter (moisture free).

Two evaluation strategies, using least squares non-linear methods, were examined to fit the experimental data: analysis of the DTG curves and the use of an optimisation algorithm (a simplified representation of the procedure performed during the parameters estimations is shown in Fig. 2). The first one considers the DTG peaks associated with the pyrolysis of the biomass components (cellulose and hemicellulose) and the shifting baseline observed due to lignin decomposition [1,18]. From the DTG curve, the corresponding points to the decomposition range of the two first pseudo-components are considered independently, in order to correlate experimental data using a first-order kinetic model (see Eq. (2)). For the lignin, a subtraction from the experimental values of the volatile matter contribution associated with the other pseudo-components is carried out. The key of the methodology is the application of a correction factor on the initial estimation of V_1^* and V_2^*, based on the probability of overlapping with the lignin devolatilisation, because the very broad range of lignin decomposition temperatures (the volatile matter generation from both hemicellulose and cellulose might be overestimated). The correction factor for each pseudo-component decomposition is calculated from the ratio between the maximum value of the simulated DTG curve and the experimental DTG value and is applied to get a new value of V_1^* and V_2^* [6,7], renamed as $(V_1^*)'$ and $(V_2^*)'$ to avoid confusion.

With the purpose to minimise errors, possibly introduced with the methodology above explained, when the derivative curve is calculated (the differential function is much more sensitive to process changes and small experimental errors or deviations can produce large errors with respect to the actual derivative curve), a second evaluation strategy was coupled to obtain the best-fit kinetic parameters (A_i, E_i, V_i^*) and to analyse the parametric dispersion. This methodology uses an optimisation algorithm to minimise the *fit* error (Eq. (3)), defined by a function related with the difference between the experimental and the simulated weight loss curve. The iterative optimisation algorithm is forced to take into account the interdependence of the kinetic parameters among pseudo-components. MATLAB 6.0 is used as the simulation tool. The differential equations are solved by a variable-order method [33] (stiff problems solver). The minimum fit is determined by a direct search method [34]. The resulting parameters with the first methodology (DTG analysis) were introduced as the starting parameters for the optimisation routine.

$$\text{fit}(\%) = \frac{100\sqrt{S_{\text{TG}}/N}}{m_0} \qquad (3)$$

Table 3 summarises the final best-fit kinetic parameters obtained with the procedure previously explained, the experimental char yields ($\eta = 100\,(m_{\text{last}}/m_0)$), the temperature for the maximum devolatilisation rate (T_{peak}), and the final *fit* error calculated according to Eq. (3) for a number of data points, N, of 82. The absolute values are showed with their standard deviations from the parametric estimation for each single curve. The experimental weight losses obtained from TGA apparatus (non-isothermal experiments) are compared with the simulated curves in Fig. 3, showing that the model successfully predicts the global mass loss process for the samples used in this work.

4.2. Comparison of isothermal experimental data with the MB model predictions

The above-mentioned MB model is based on a superposition of kinetics of the primary components of biomass: cellulose, hemicellulose, and lignin. All three reactions schemes are based on the model proposed by Bradbury et al. [35] for the cellulose decomposition (see Fig. 4). The initialisation reaction (k_1) does not produce any mass change. In addition, all reactions are defined as irreversible first-order processes. The ordinary differential equations which describe the MB kinetic scheme are:

$$\frac{\mathrm{d}(y_{\text{comp}})}{\mathrm{d}t} = -k_1 y_{\text{comp}} \qquad (4)$$

$$\frac{\mathrm{d}(y_{\text{a}})}{\mathrm{d}t} = k_1 y_{\text{comp}} - (k_2 + k_3)y_{\text{a}} \qquad (5)$$

$$\frac{\mathrm{d}(y_{\text{t}})}{\mathrm{d}t} = k_2 y_{\text{a}} \qquad (6)$$

$$\frac{\mathrm{d}(y_{\text{c}})}{\mathrm{d}t} = x\,k_3\,y_{\text{a}} \qquad (7)$$

$$\frac{\mathrm{d}(y_{\text{g}})}{\mathrm{d}t} = (1-x)k_3 y_{\text{a}} \qquad (8)$$

where y_{comp}, y_{a}, y_{t}, y_{c}, and y_{g} correspond, respectively, to the weight fractions of virgin component, activate component, condensable products, char as a product of the competitive reactions, and gas. The char formation mass ratios for the reaction k_3 are: 0.60 (hemicellulose), 0.35 (cellulose), and 0.75 (lignin). These values were proposed by Miller and Bellan taking into account results obtained in previous studies [12,24].

The kinetic parameters for cellulose are taken to be identical to those used by Di Blasi and Russo [36] while the hemicellulose and lignin parameters are modified from previous schemes to fit the results of several experiments for beech wood, lignin and maple wood pyrolysis [14] (no additional information is reported by the authors about the methodology followed in the parametric determination process). The MB model parameters are provided in Table 4.

On the other hand, it is necessary to clearly define the residual weight fraction in moisture-free basis (w) which corresponds to the experimental value obtained at the end of an isothermal run. In this sense, the w value can be calculated from the MB model
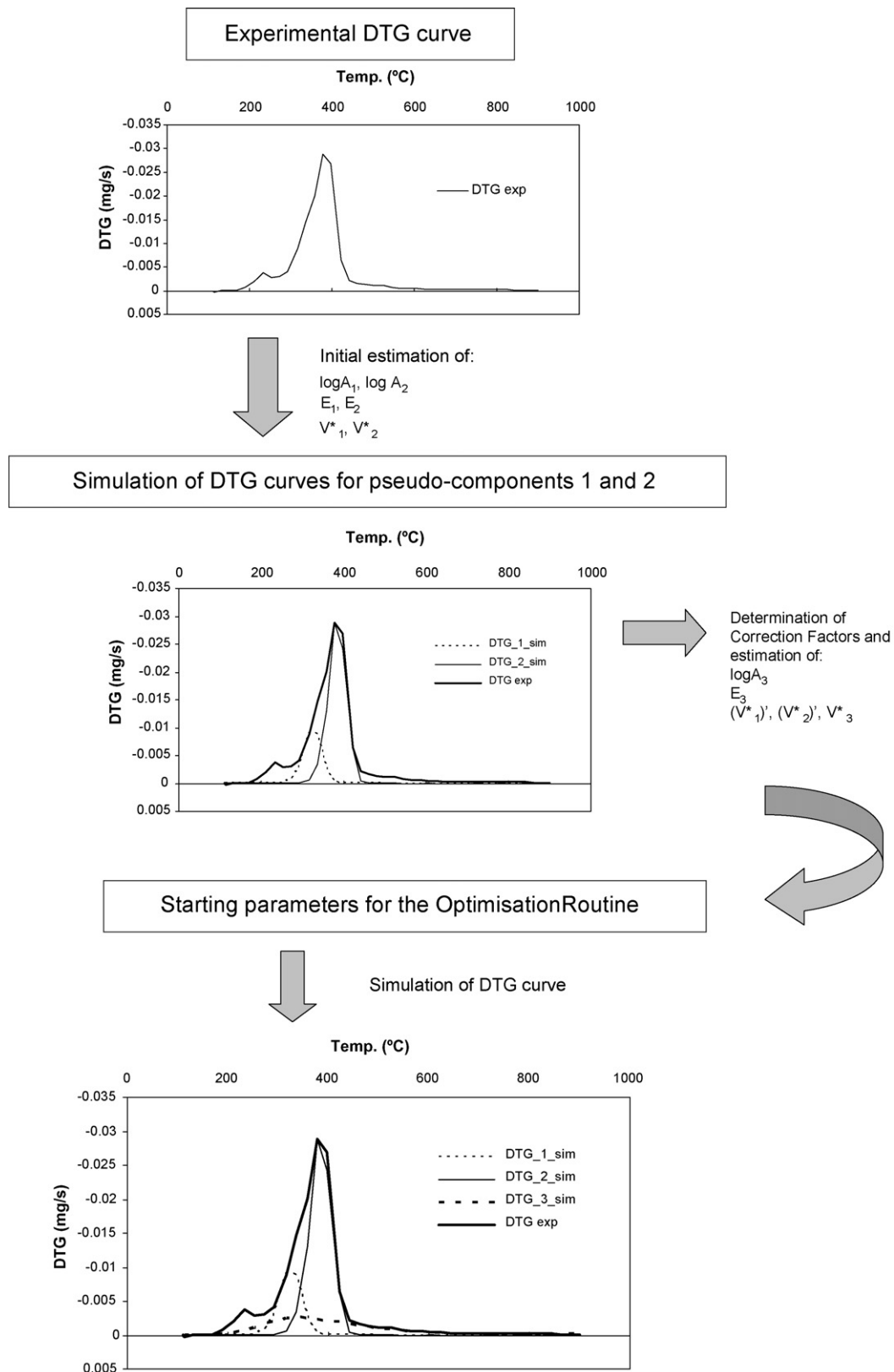
Fig. 2. Simplified scheme of the procedure performed during the kinetic parameters estimation from TGA data.

Table 3
Kinetic parameters of the model based on superimposed pseudo-components and deduced from TGA experiments

	Pseudo-component			Fit (%)	η (%)	T_{peak} (K)
	First	Second	Third			
Untreated bagasse						
$\log A_i$ (s^{-1})	15.67 ± 0.1	18.00 ± 0.0	2.58 ± 0.1	1.17	23.1	643
E_i (kJ/mol)	198.00 ± 0.9	246.50 ± 0.2	57.30 ± 0.0			
V_i^*/m_0	0.141 ± 0.01	0.435 ± 0.02	0.190 ± 0.01			
Washed bagasse						
$\log A_i$ (s^{-1})	15.43 ± 0.1	18.09 ± 0.0	2.28 ± 0.2	0.89	16.2	683
E_i (kJ/mol)	202.40 ± 0.6	253.50 ± 0.4	52.30 ± 3.4			
V_i^*/m_0	0.177 ± 0.01	0.418 ± 0.01	0.252 ± 0.02			

as follows:

$$w(t) = \sum_{i=1}^{3} c_i [1 - y_t(t) - y_g(t)]_i \qquad (9)$$

Fig. 4. Generic reaction scheme to model cellulose, hemicellulose and lignin kinetics used by Miller and Bellan.
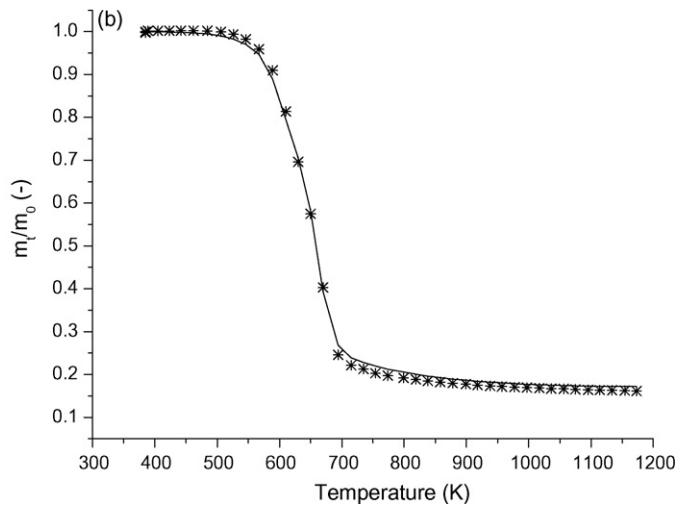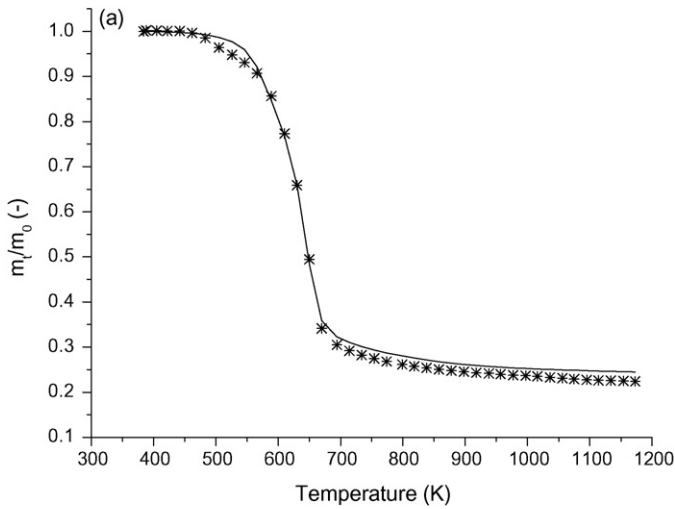
Fig. 3. TG curves during pyrolysis of the untreated (a) and water-washed (b) sugar cane bagasse. The symbols are experimental data; the solid line curves are predictions from the model (Eq. (2)) using parameters reported in Table 3.
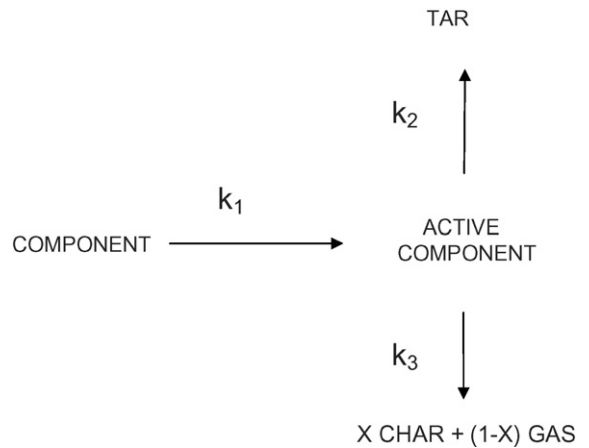
The term c_i represents the weight fraction of the corresponding biomass components in the virgin materials. For the material analysed in this work, a method suggested by Orfao et al. [3] which approximately estimates the content of the biomass components was applied [3,37]. In this way, the mass fractions of hemicellulose, cellulose and lignin may be estimated by means of the following equations:

$$c_1 = \frac{V_1^*/m_0}{0.717} \qquad (10)$$

$$c_2 = \frac{V_2^*/m_0}{0.802} \qquad (11)$$

$$c_3 = 1 - c_1 - c_2 - x_{ext} \qquad (12)$$

Table 4
Reaction parameters of the MB model

Reaction	$\log A$ (s^{-1})	E (kJ/mol)
k_1 (cel.)	19.45	242.4
k_2 (cel.)	14.52	196.5
k_3 (cel.)	10.11	150.5
k_1 (hem.)	16.32	186.7
k_2 (hem.)	15.94	202.4
k_3 (hem.)	11.41	145.7
k_1 (lig.)	8.98	107.6
k_2 (lig.)	9.18	143.8
k_3 (lig.)	6.89	111.4

where V_1^* and V_2^* are the optimised parameters summarised in Table 3 and the values 0.717 and 0.802 correspond, respectively, to the fractions of hemicellulose and cellulose which decompose in the temperature range corresponding to pseudo-components 1 and 2. These values were estimated by Orfao et al. [3] taking into consideration the average between the experimental values obtained in air and nitrogen for xylan (considered to be representative of the hemicellulose) and for cellulose (Avicel cellulose PH-101). The mass fraction of extractives was taken into account when the mass fraction of lignin was estimated (for the material analysed in the present study, $x_{ext} = 0.021$).

A hyperbolic tangent function was used to model the temporal evolution of the sample temperature (T_1). The parameters of this function were adjusted from the data obtained during the characterisation of the heating dynamics of the reactor. According with this procedure, the evolution of T_1 can be simulated as follows:

$$T_1 = T_1^* \left(\frac{e^{0.15t} - 1}{e^{0.15t} + 1} \right) \tag{13}$$

In order to ensure the reliability of the experimental results as a previous step to evaluate the ability of the MB model, a preliminary interpretation and analysis of the data should be conducted. The goal of this procedure was to verify that the secondary char formation was negligible. Fig. 5 shows the pyrolysis curve as a function of both temperature and solid residence time for the untreated and water-washed bagasse samples. As can be shown, the pyrolysis rate reaches significant values above 550 K for the untreated bagasse samples and 570 K for the washed ones. This temperature variation can be related to a kinetic effect, which is explained by the inorganic matter originally present in the biomass samples. As the temperature increases, the conversion level becomes independent of the solid residence time and at temperatures above 650 K the devolatilisation rate is very low. On the other hand, the final residual fraction or char yield slowly decreases as temperature increases. This fact can suggest that an increase in the temperature promotes the production of volatiles rather than char if a competitive kinetic scheme between the weight-loss reactions and the char formation reactions is assumed. To complete the interpretation of the data displayed in Fig. 5, a fixed carbon determination by TGA was performed for each char obtained. The evolution of the fixed carbon content seems to indicate that the role played by the secondary charring reactions is negligible because no increase of the degree of carbonisation with the solid residence time (at temperatures above 650 K) was observed.

A comparison of the MB model predictions with the isothermal experiments is made in Figs. 6 and 7. The agreement between the MB model predictions and experiments was
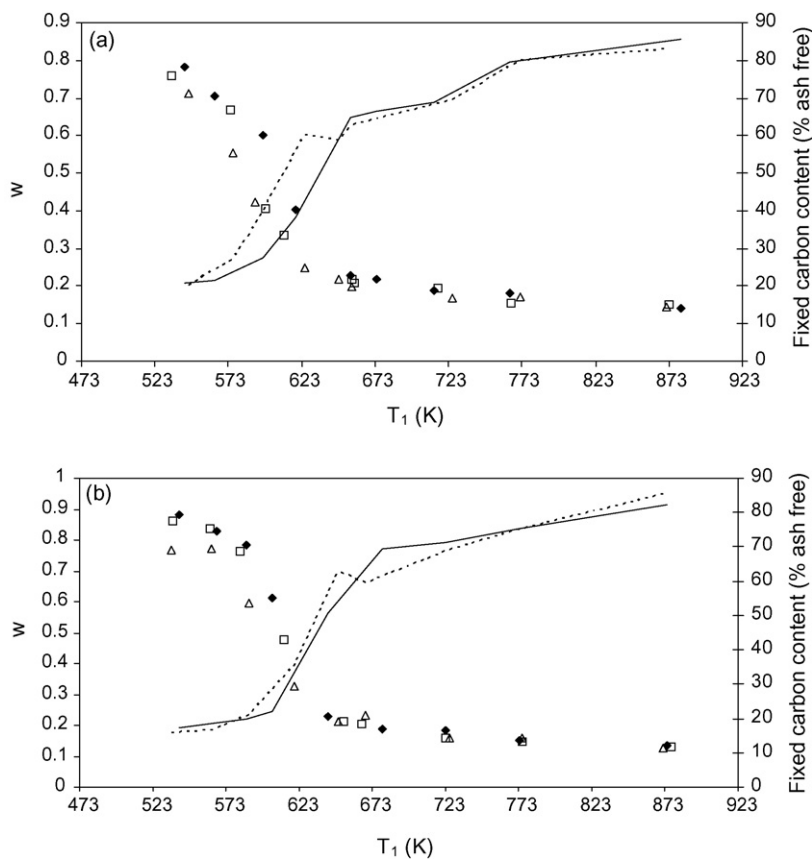

Fig. 5. Isothermal char yields as a function of temperature and solid residence time for the (a) untreated bagasse and (b) water-washed bagasse. The symbols represent the experimental measures of the residual weight fraction: (diamond), $\tau = 3$ min; (square), $\tau = 6$ min; (triangle), $\tau = 8$ min. The lines represent the measured fixed carbon content: (solid line), $\tau = 3$ min; (dotted line), $\tau = 8$ min.
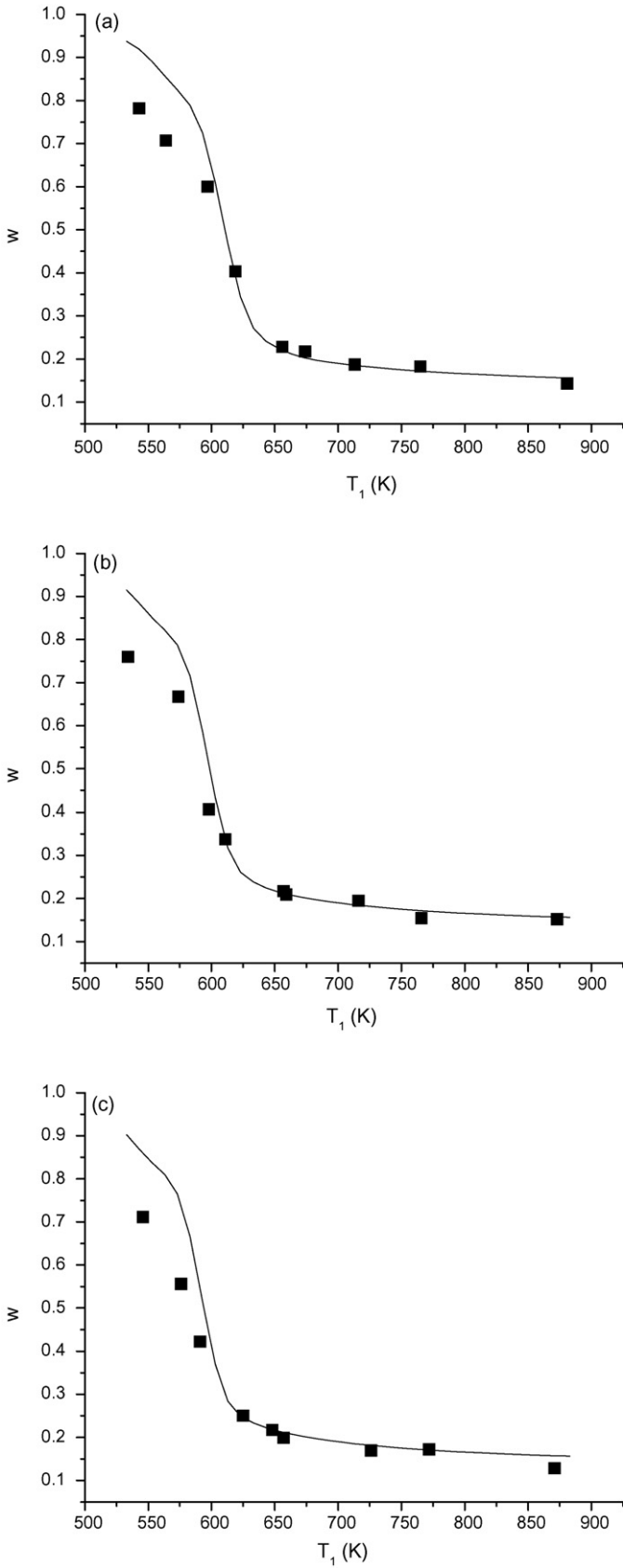
Fig. 6. Isothermal mass-change determination of untreated sugar cane bagasse. The curves predicted by the MB model in comparison with experimental points corresponding to (a) $\tau = 3$ min, (b) $\tau = 6$ min, and (c) $\tau = 8$ min.
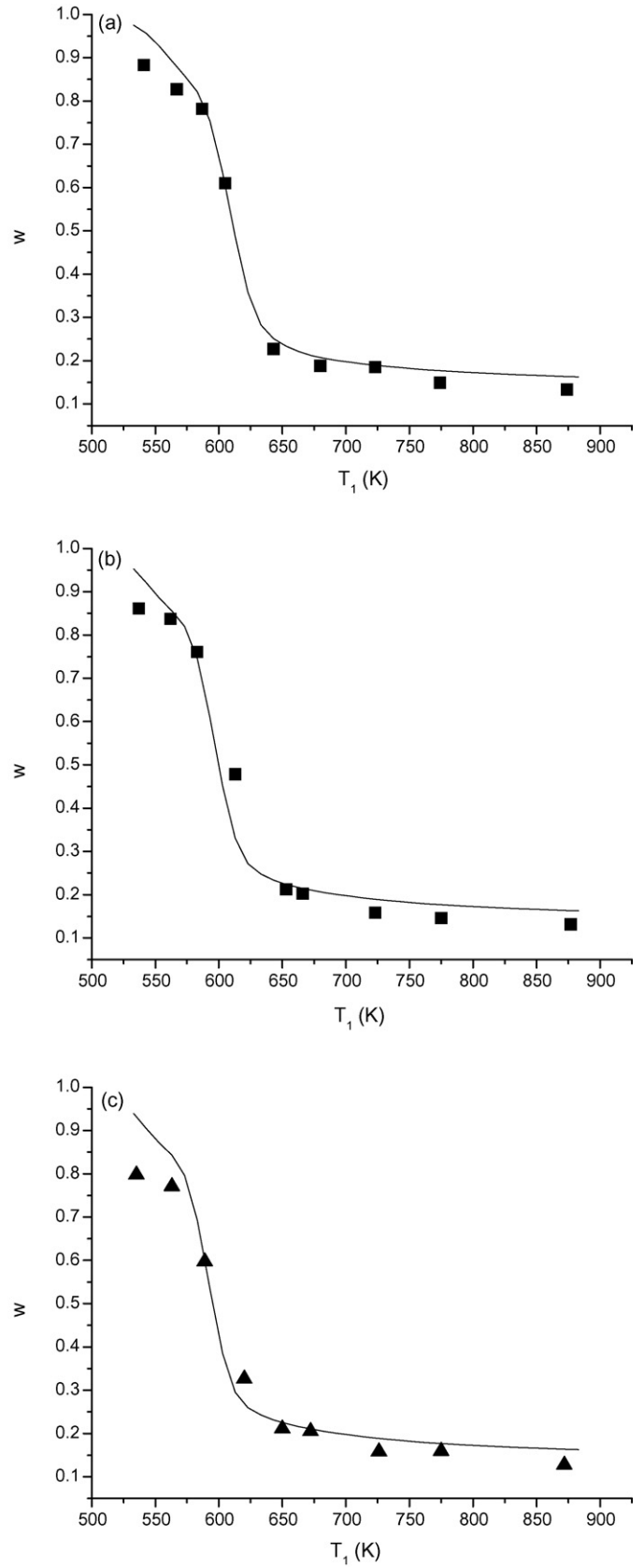

Fig. 7. Isothermal mass-change determination of washed sugar cane bagasse. The curves predicted by the MB model in comparison with experimental points corresponding to (a) $\tau = 3$ min, (b) $\tau = 6$ min, and (c) $\tau = 8$ min.
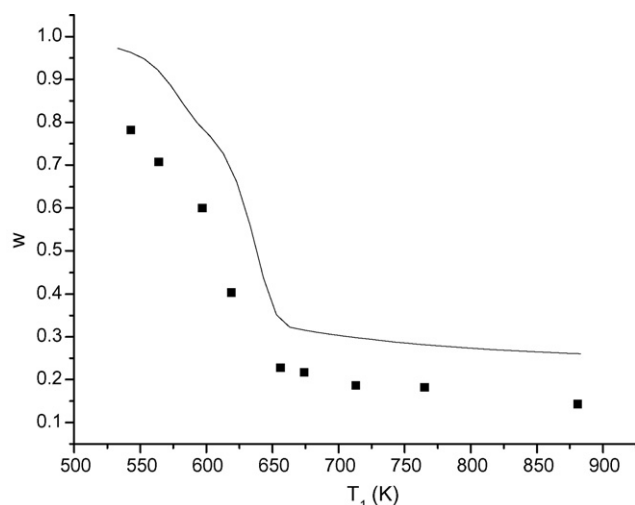
Fig. 8. Isothermal mass-change determination of untreated sugar cane bagasse ($\tau = 3$ min). The symbols represent the experimental measurements. The solid line represents the mass predictions using the model deduced from TGA data at 20 K min^{-1}.

acceptable. However, there are some deviations: the pyrolysis initialisation temperature was over-predicted by the MB model (especially for the untreated bagasse samples) and the final residual fraction was slightly overestimated for the treated bagasse. Among several factors related to the systematic errors and additional uncertainties related to the procedure used to estimate the biomass composition (c_1, c_2, and c_3), the catalytic effect of the mineral matter on final char and pyrolysis rate could explain the observed deviations between the MB model predictions and the isothermal measurements. In fact, the MB model only considered "typical" (i.e., untreated) biomass samples.

4.3. Application of the proposed model for isothermal mass-change determination

In this point, the isothermal results were compared with those obtained using the kinetic model according to Eq. (2). An excellent qualitative agreement was observed, but with a near constant over-prediction in magnitude (see Fig. 8 as an example). This trend is encouraging to test the ability of the adjusted TGA model to reproduce the isothermal results. The parameters of the TGA model were adjusted following the criteria explained in Section 3. In this sense, the modifiable kinetic parameters (V_i^* and $\log A_i$), deduced from TGA experiments performed at 20 K min^{-1}, were adjusted to obtain a qualitative visual agreement between calculated and observed data. In other words, no heuristic processes have been proposed to optimise the modifiable parameters to obtain the best agreement between calculated and observed points. We believe that this task should be taken into account in future works when more information from further studies (involving the application of the proposed methodology for different biomass samples) is available.

Table 5 shows the new kinetic parameters applied to simulate the isothermal experiments. It is interesting to note that the variation of initial kinetic parameters was the same for all pseudo-components. These variation percentages can be explained taking into account the operating conditions and biomass composition. In this sense, the increase of the pre-exponential factors (keeping constant the apparent activation energy values) should be considered as an effective means to minimise the impact of an increase of the thermal lag (difference between the real and measured temperature) inherent to fast heating rates. On the other hand, the expected increase of the normalised volatile productions (V_i^*/m_0) is related to the effect of the heating regime: the isothermal experiments were performed with relatively high-heating rates (>300 K min^{-1}) and, consequently, the low-temperature contributions to the pyrolysis (characterised by a lower devolatilisation rate) become less significant. Special attention should be given to differences in the volatile yields between untreated and washed bagasse. This fact could be related to the mineral matter present in the sugar cane bagasse, which catalyses the pyrolytic decomposition in an unpredictable variety of ways. This catalytic effect can play a major role for the isothermal experiments.

A contrast between the proposed model predictions and experimental data is displayed in Figs. 9 and 10. As a subjectively reasonable conclusion from analysing the results we mention the fact that the proposed model reproduces the isothermal mass-change more accurately than the MB model from qualitative point of view. One explanation for this fact is that the kinetic parameters have been deduced independently for each sample (untreated and washed bagasse) and, consequently, the effect of the inorganic matter has been intrinsically included in the kinetic scheme.

Table 5
Kinetic parameters of the adjusted TGA model

	Pseudo-component 1	Pseudo-component 2	Pseudo-component 3	Percentage of variation[a]
Untreated bagasse				
$\log A_i$ (log s^{-1})	16.45	18.90	2.71	+5
E_i (kJ/mol)	198.0	246.5	57.3	0
V_i^*/m_0	0.155	0.479	0.209	+10
Water-washed bagasse				
$\log A_i$ (log s^{-1})	16.45	18.90	2.40	+5
E_i (kJ/mol)	202.4	253.5	52.3	0
V_i^*/m_0	0.186	0.439	0.265	+5

[a] Percentage of variation of the initial kinetic parameters (deduced from TGA experiments performed at 20 K min^{-1}) for all pseudo-components.
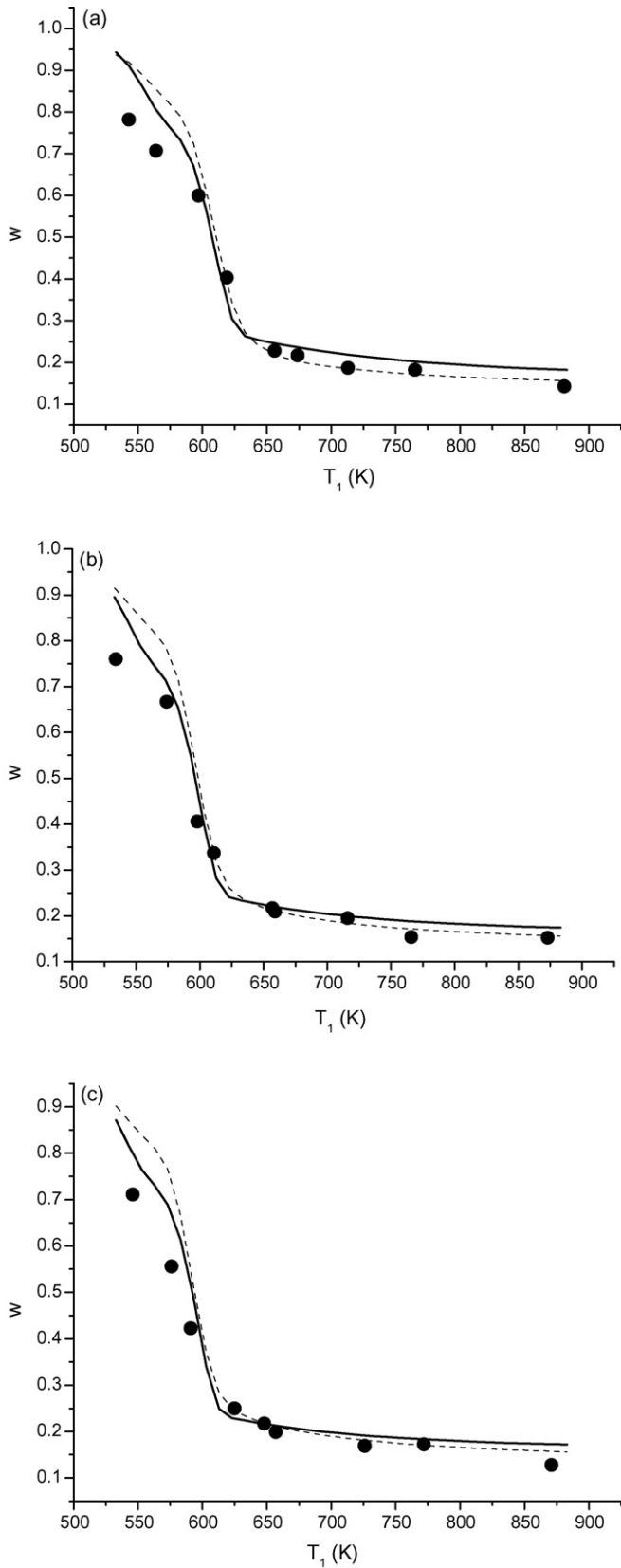
Fig. 9. Isothermal mass-change determination of untreated sugar cane bagasse. The curves predicted by the proposed model (solid line) and the MB model (dashed line) in comparison with experimental points corresponding to (a) $\tau = 3$ min, (b) $\tau = 6$ min, and (c) $\tau = 8$ min.
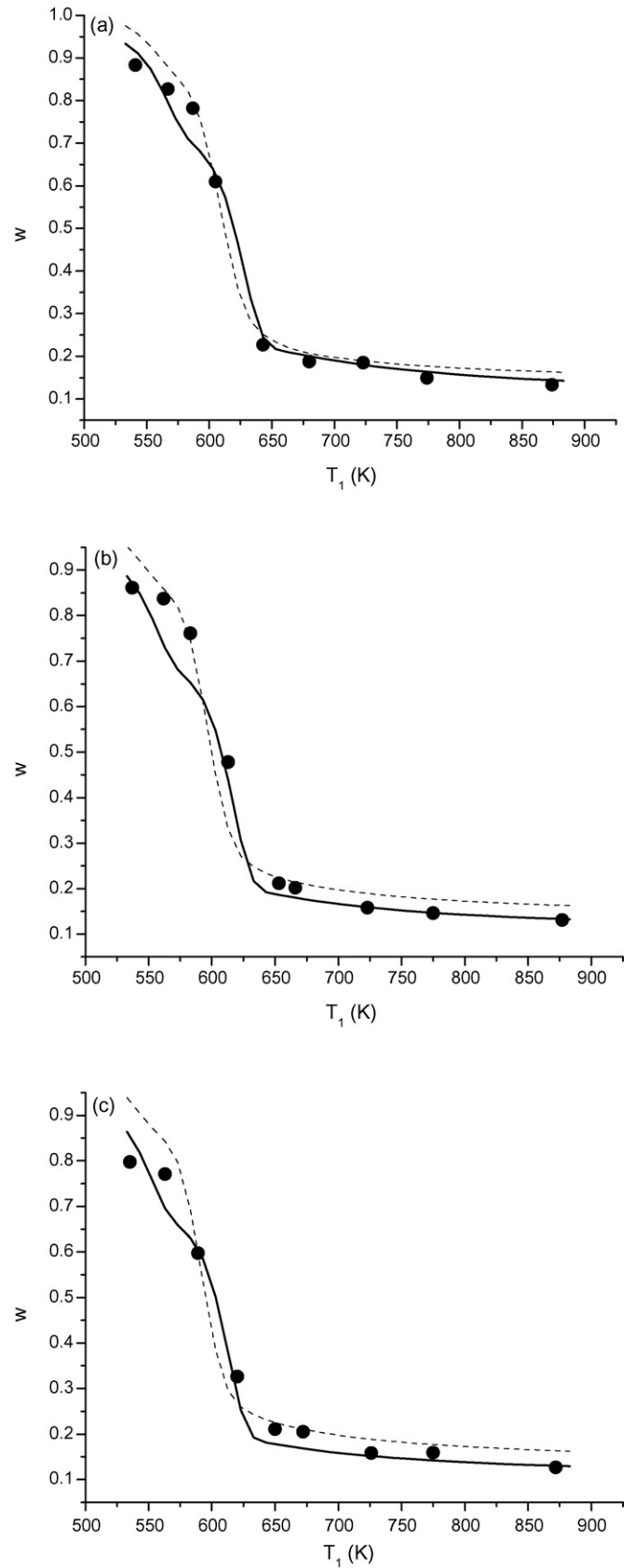
Fig. 10. Isothermal mass-change determination of washed sugar cane bagasse. The curves predicted by the proposed model (solid line) and the MB model (dashed line) in comparison with experimental points corresponding to (a) $\tau = 3$ min, (b) $\tau = 6$ min, and (c) $\tau = 8$ min.

5. Conclusions

A new kinetic approach is presented for modeling micro-particle (kinetically controlled) pyrolysis of a sample of sugar cane bagasse for isothermal conditions. The kinetic model is based on a superimposition of kinetics pseudo-components linked to hemicellulose, cellulose, and lignin. All three kinetic schemes are based on single-step reactions to model primary pyrolysis. In this sense, the experimental conditions were effective in minimising heat transfer intrusions and vapour–solid interactions (to avoid secondary char formation).

The kinetic model based on superimposed pseudo-components was previously deduced from thermogravimetric data obtained at $20\,\mathrm{K\,min^{-1}}$. The potential effects related to an increase of the heating rate and the mineral matter content were taken into account during the adjustment of the kinetic parameters to reproduce the isothermal experiments.

The robust MB kinetic model was selected in order to compare the degree of agreement between the two models. In the MB kinetic scheme, the pyrolysis of general biomass materials is modeled with multi-step kinetics involving competitive primary decomposition reactions. Although the MB model has been proven effective enough to reproduce the mass-change curve corresponding to the isothermal experiments, a better performance was achieved for the model proposed in this work. The higher prediction accuracy can be due to the fact that the effect of the inorganic matter has been intrinsically included in the proposed kinetic model.

The results of this study suggest the possibility of developing a new methodology for estimating the isothermal mass-change curve in order to predict the behaviour of biomass feeds in combustors and gasifiers. In other words, the procedures followed in the present study for sugar cane bagasse samples could be useful to predict the isothermal pyrolysis behaviour of arbitrary biomass feedstocks. Further studies with different biomass samples would be interesting to analyse the kinetic approach capabilities. On the other hand, additional research works should contemplate the incorporation of the kinetic model into a porous particle model to simulate the macro-particle pyrolysis. At this point, studies involving the addition of the secondary charring reactions in the kinetic scheme should be considered.

Acknowledgements

References

[1] M.J. Antal, G. Várhegyi, Cellulose pyrolysis kinetics: the current state of knowledge, Ind. Eng. Chem. Res. 34 (1995) 703–717.

[2] H. Teng, Y.C. Wei, Thermogravimetric studies on the kinetics of rice hull pyrolysis and the influence of water treatment, Ind. Eng. Chem. Res. 37 (1998) 3806–3811.

[3] J.J.M. Orfao, F.J.A. Antunes, J.L. Figueiredo, Pyrolysis kinetics of ligno-cellulosic materials—three independent reactions model, Fuel 78 (1999) 349–358.

[4] L. Sorum, M.G. Gronli, J.E. Hustad, Pyrolysis characteristics and kinetics of municipal solid wastes, Fuel 80 (2001) 1217–1227.

[5] E. Biagini, F. Lippi, L. Petarca, L. Tognotti, Devolatilization rate of biomasses and coal-biomasses blends: an experimental investigation, Fuel 81 (2002) 1041–1050.

[6] J.J. Manyà, E. Velo, L. Puigjaner, Kinetics of biomass pyrolysis: a reformulated three-independent-reactions model, Ind. Eng. Chem. Res. 42 (2003) 434–441.

[7] C.J. Gómez, J.J. Manyà, E. Velo, L. Puigjaner, Further applications of a revisited summative model for kinetics of biomass pyrolysis, Ind. Eng. Chem. Res. 43 (2004) 901–906.

[8] F. Shafizadeh, P.P.S. Chin, Thermal deterioration of wood, ACS Symp. 43 (1977) 57–67.

[9] F. Thurner, U. Mann, Kinetic investigation of wood pyrolysis, Ind. Eng. Chem. Proc. Des. Dev. 20 (1981) 482–488.

[10] D.S. Scott, J. Piskorz, The flash pyrolysis of aspen-poplar wood, Can. J. Chem. Eng. 60 (1982) 666–674.

[11] A.G. Liden, F. Berruti, D.S. Scott, A kinetic model for the production of liquids from the flash pyrolysis of biomass, Chem. Eng. Commun. 65 (1988) 207–221.

[12] C.A. Koufopanos, N. Papayannakos, G. Maschio, A. Lucchesi, Modeling of the pyrolysis of biomass particles. Studies on kinetics, thermal and heat transfer effects, Can. J. Chem. Eng. 69 (1991) 907–915.

[13] C. Di Blasi, Kinetic and heat transfer control in the slow and flash pyrolysis of solids, Ind. Eng. Chem. Res. 35 (1996) 37–46.

[14] R.S. Miller, J. Bellan, A generalized biomass pyrolysis model based on superimposed cellulose, hemicellulose and lignin kinetics, Combust. Sci. Technol. 126 (1997) 97–137.

[15] C. Di Blasi, C. Branca, Kinetics of primary product formation from wood pyrolysis, Ind. Eng. Chem. Res. 40 (2001) 5547–5556.

[16] G. Várhegyi, M.J. Antal, T. Szekely, F. Till, E. Jakab, Simultaneous thermogravimetric-mass spectrometric studies of the thermal decomposition of biopolymers. 2. Sugar cane bagasse in the presence and absence of catalysts, Energy Fuels 2 (1988) 273–277.

[17] O. Faix, E. Jakab, F. Till, T. Szekely, Study on low mass thermal degradation products of milled woods lignins by thermogravimetry-mass spectrometry, Wood Sci. Technol. 22 (1988) 323–334.

[18] G. Várhegyi, M.J. Antal, T. Szekely, P. Szabo, Kinetics of the thermal decomposition of cellulose, hemicellulose, and sugar cane bagasse, Energy Fuels 3 (1989) 329–335.

[19] R.J. Evans, T.A. Milne, Molecular characterization of the pyrolysis of biomass. 1. Fundamentals, Energy Fuels 1 (1987) 123–137.

[20] G. Várhegyi, E. Jakab, M.J. Antal, Is the Broido-Shafizadeh model for cellulose pyrolysis true? Energy Fuels 8 (1994) 1345–1352.

[21] G. Várhegyi, M. Gronli, C. Di Blasi, Effects of sample origin, extraction, and hot-water washing on the devolatilization kinetics of chestnut wood, Ind. Eng. Chem. Res. 43 (2004) 2356–2367.

[22] C. Di Blasi, C. Branca, A. Santoro, R.A.P. Bermudez, Weight loss dynamics of wood chips under fast radiative heating, J. Anal. Appl. Pyrol. 57 (2001) 77–90.

[23] C. Di Blasi, C. Branca, A. Santoro, E.G. Hernandez, Pyrolytic behavior and products of some wood varieties, Combust. Flame 124 (2001) 165–173.

[24] R.S. Miller, J. Bellan, Analysis of reaction products and conversion time in the pyrolysis of cellulose and wood particles, Combust. Sci. Technol. 119 (1996) 331–373.

[25] D.S. Scott, L. Paterson, J. Piskorz, D. Radlein, Pretreatment of poplar wood for fast pyrolysis: rate of cation removal, J. Anal. Appl. Pyrol. 57 (2000) 169–176.

[26] G. Várhegyi, M.J. Antal, E. Jakab, P. Szabo, Modeling of biomass pyrolysis, J. Anal. Appl. Pyrol. 42 (1997) 73–80.

[27] M. Stenseng, A. Jensen, K. Dam-Johansen, Investigation of biomass pyrolysis by thermogravimetric analysis and differential scanning calorimetry, J. Anal. Appl. Pyrol. 58 (2001) 59–765.

[28] G.M. Simmons, M. Gentry, Particle size limitations due to heat transfer in determining pyrolysis kinetics of biomass, J. Anal. Appl. Pyrol. 10 (1986) 117–127.

[29] D.S. Scott, J. Piskorz, M.A. Bergougnon, R. Graham, R.P. Overend, The role of temperature in the fast pyrolysis of cellulose and wood, Ind. Eng. Chem. Res. 27 (1988) 8–15.

[30] C.A. Koufopanos, G. Maschio, A. Lucchesi, Kinetic modelling of the pyrolysis of biomass and biomass components, Can. J. Chem. Eng. 67 (1989) 75–84.

[31] G. Várhegyi, P. Szabó, E. Jakab, F. Till, Least squares criteria for the kinetics evaluation of thermoanalytical experiments. Examples from a char reactivity study, J. Anal. Appl. Pyrol. 57 (2001) 203–222.

[32] W.S. Mok, M.J. Antal, P. Szabó, G. Várhegyi, Formation of charcoal from biomass in a sealed reactor, Ind. Eng. Chem. Res. 31 (1992) 1162–1166.

[33] L.F. Shampine, M.W. Reichelt, The MATLAB ONE suite, SIAM J. Sci. Comput. 18 (1997) 1–22.

[34] J.C. Lagarias, J.A. Reeds, M.H. Wright, P.E. Wright, Convergence properties of the Nelder-Mead simplex method in low dimensions, SIAM J. Optim. 9 (1998) 112–147.

[35] A.G. Bradbury, Y. Sakai, F. Shafizadeh, A kinetic model for pyrolysis of cellulose, J. Appl. Polym. Sci. 23 (1979) 3271–3280.

[36] C. Di Blasi, G. Russo, Modeling of transport phenomena and kinetics of biomass pyrolysis, in: A.V. Bridgwater (Ed.), Advances in Thermochemical Biomass Conversion, vol. 2, Blackie Academic & Professional, New York, 1994, pp. 906–921.

[37] J.J. Manyà, Contribució a l'estudi de la cinètica de la piròlisi primària de materials lignocel·lulòsics per a diferents règims d'escalfament, Ph.D. Thesis, Universitat Politècnica de Catalunya, Barcelona, Spain, in press.